ACS OMEGA

Open Access

http://pubs.acs.org/journal/acsodf

Article

Bimetallic Cu–Zn Zeolitic Imidazolate Frameworks as Peroxidase Mimics for the Detection of Hydrogen Peroxide: Electrochemical and Spectrophotometric Evaluation

Aswathi Mechoor, Sheela Berchmans,* and Ganesh Venkatachalam*

Cite This: *ACS Omega* 2023, 8, 39636–39650

Read Online

ACCESS | Metrics & More | Article Recommendations | Supporting Information

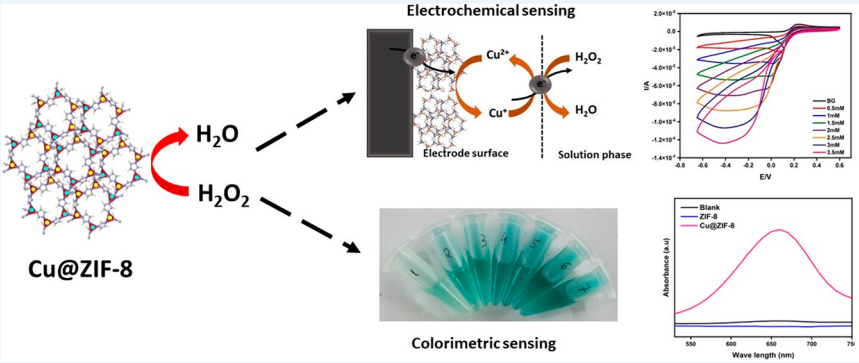

ABSTRACT: A copper incorporated zeolitic imidazolate framework-8 (ZIF-8) has been synthesized and demonstrated to be a potential material for a peroxidase mimic. The resultant bimetallic Cu–Zn incorporated MOF is used for the dual mode sensing of hydrogen peroxide by following electrochemical as well as spectrophotometric methods. Using 3,3′,5,5′-tetramethylbenzidine (TMB) as a chromogenic substrate, spectrophotometric studies are carried out, and the steady state kinetic parameters are determined for two different concentrations of Cu incorporated ZIF-8 (viz Cu@ZIF-8-1 and Cu@ZIF-8-2). It is found that both Cu@ZIF-8-1 and Cu@ZIF-8-2 exhibit more affinity toward the TMB substrate than the *horseradish peroxidase* (HRP) enzyme as indicated by the low K_m values obtained for the substrate. Also, as the concentration of incorporated Cu increases, V_{max} values are also found to be enhanced. Electrochemically, the Cu@ZIF-8 modified glassy carbon electrode (GCE) showed a good response for peroxide detection in the concentration range from 0.5 mM to 5 mM at a working potential of −0.25 V in PBS (pH 7.0) with a limit of detection (LOD) value of 0.46 mM and a sensitivity of 20.25 μA/mM. Further, the chromogenic substrate TMB is successfully immobilized on the electrode surface and subsequently used for the peroxide detection along with Cu@ZIF-8. Here, TMB acts as a mediator and shifted the working potential to 0.1 V in acetate buffer (pH 5.0) in the concentration range from 0.5 mM to 5 mM with an LOD value of 0.499 mM and a sensitivity of 0.097 μA/mM. Interestingly, the same electrode in PBS of pH 7.0 showed a response to peroxide at a working potential of −0.1 V in the concentration range from 0.5 mM to 5 mM with an LOD value of 0.143 mM and a sensitivity of 0.33 μA/mM. Moreover, the applicability of this material for peroxide sensing is evaluated using milk samples, and the proposed material is able to recover the peroxide present in milk. Thus, the bimetallic Cu–Zn MOF can be utilized for the dual mode sensing of peroxide and can be extended for various real time applications.

1. INTRODUCTION

One of the most important biomacromolecules, namely enzymes are biocatalysts that can catalyze biological reactions in living organisms as well as several commercially important reactions.[1] Substrate specificity and high catalytic efficiency make them an ideal material for biosensing applications. But protein-based structures of the enzymes make them highly vulnerable to harsh environmental conditions that causes their denaturation. Moreover, high production cost and specific storage conditions make them disadvantageous for real time application.[2] To overcome these short comings, materials that can mimic the properties of natural enzymes in terms of structure and function are being developed. These kinds of materials that can mimic the properties of natural enzymes are known as enzyme mimics. High stability to harsh conditions, ease of production, low cost associated with synthetic procedures, easy storage, wide pH range tolerance, and

Received: July 29, 2023
Accepted: September 26, 2023
Published: October 15, 2023

reusability make them highly advantageous over the natural enzymes.[2] However, enzyme mimics could not attain the same catalytic efficiency and biocompatibility as those of the natural enzymes. Hence, materials that can match the catalytic efficiency of the natural enzymes along with better biocompatibility need to be developed.[3] The common enzyme mimicking materials that have been often explored as enzyme mimicking reagents are metal nanoparticles (Pt, Ag, Au), metal oxides (V_2O_5, Fe_3O_4, CeO_2), carbon based materials (CNT, GO, fullerene), Prussian blue, metal hydroxides, etc.[4]

Peroxidases are the natural enzymes, possessing the capability to catalyze various oxides and peroxides.[5] Their high catalytic efficiency and specificity make them advantageous for applications like biosensing, food processing, disease diagnosis, medicine, wastewater treatment, etc.[6] One such enzyme that belongs to the ferroprotoporphyrin group of peroxidases is *horseradish peroxidase* (HRP). It is characterized by its high sensitivity, rapid analysis, and low background interferences.[7] However, the natural HRP enzyme is highly vulnerable to harsh environmental conditions. Also, it is expensive, and the procedures used for the preparation and purification are complicated, which limits its wide range of applications.[8] As stated earlier, in order to overcome the limitations of this natural HRP enzyme, many peroxidase mimicking materials are being developed. These materials are expected to possess high stability, reusability, ease of storage and handling, and simple synthesis procedures. These peroxidase mimics can be used for the sensing of various analytes like H_2O_2, glucose, cholesterol, cysteine, melamine, protein, dopamine, urea, leukemia cancer cells, and so on.[7]

One of the emerging enzyme mimicking materials is metal organic frameworks (MOFs). Basically, MOFs are organic−inorganic hybrids formed by the coordination between a metal ion and a tunable organic ligand resulting in the formation of 2D or 3D extended structures.[9] High surface area, tunable porosity, thermal and chemical stability, biocompatibility, and unique surface topology are the major characteristics of these coordination networks which enable their utilization in various applications like biosensing, catalysis, gas separation, drug delivery, etc.[9] There are several reports on using MOFs as enzyme mimicking materials.[6,10−12] Mostly MOFs based on Fe, Cu, Ce, Zr, etc. are found to exhibit the enzyme mimicking properties.[2] A Cu-based MOF was found to display intrinsic peroxidase like activity, which was further utilized for glucose detection as well.[12] MIL-53, an iron based MOF, was also found to have intrinsic peroxidase-like activity and used for sensing of peroxide and ascorbic acid.[13] Multimetallic MOFs are also shown to be highly advantageous as the enzyme mimicking materials. These kinds of MOFs will have multiple active sites that will enhance their catalytic activity and performance. Also, doping of MOFs with various metals can enhance the performance of Fenton or Fenton-like reactions and thus enhance the decomposition efficiency of H_2O_2. Molybdenum (Mo) was doped over a copper-2-methyimidazole (2-MI) MOF where the doping of Mo was proven to enhance the peroxidase mimicking activity of Cu-2-MI MOF.[14] An Fe−Ni-based bimetallic MOF was found to have intrinsic peroxidase-like activity, and it was immobilized along with the *glucose oxidase* enzyme for glucose sensing.[15] Doping of copper to the ZIF-67 MOF was shown to enhance gas uptake capacity and reported to be utilized for organic dye degradation.[16]

The zeolitic imidazolate framework (ZIF) is a subclass of MOFs, which consists of an imidazolate organic ligand linked to a metal ion. This metal ion can be mainly Zn (ZIF-8) or Co (ZIF-67). ZIFs possess a zeolite kind of structure in which comparatively the metal ion plays the role of silicon and bridging imidazolate anions play the role of oxygen. Their high porosity, crystallinity, surface area, tunable size, and good stability make them highly attractive for various applications.[17,18] Despite their advantages, it is highly desirable to modify the ZIF-based materials further with metal ions like Cu, Ni, Cd, etc. in order to create multimetallic systems. These multimetallic ZIFs will have better activity compared to parent ZIFs. Synthetic flexibility of these materials will allow the incorporation of metal ions without disrupting the structure.[19,20]

Hydrogen peroxide (H_2O_2) is one of the most extensively studied bioanalytes, and its detection is of high importance in the clinical, food, and cosmetic industries. H_2O_2 is usually used as a preservative in milk and milk products in order to avoid spoilage. The addition of H_2O_2 prevents the microbial growth that leads to milk spoilage. But excessive quantities of H_2O_2 are highly harmful to human health. They will cause diseases related to oxidative stress like cancer and cardiovascular diseases, Alzheimer's, etc. Hence, it is highly necessary to monitor the quantity of H_2O_2, especially in milk, to monitor its quality as well health standards. This detection can be carried out by various techniques like spectrophotometry, electrochemistry, chemiluminescence, HPLC, and fluorescence spectrometry.[21,22]

Detection of H_2O_2 is usually carried out using a simple peroxidase assay that is performed using a chromogenic substrate along with HRP and H_2O_2, which is monitored using optical spectroscopy techniques. Several compounds such as 3,3′,5,5′-tetramethylbenzidine (TMB), 2,2′-azino-di(3-ethylbenzthiazoline) sulfonic acid (ABTS), o-phenylenediamine (OPD), and 3,3′-diaminobenzidine (DAB) are used as the major chromogenic substrates for the peroxidase assay. But TMB is considered one of the most attractive owing to its better sensitivity compared to ABTS and OPD as well as it being neither mutagenic nor carcinogenic. H_2O_2 acts as the oxidizing agent for HRP and initiates the HRP redox cycle. The oxidized HRP will in turn oxidize TMB into a blue-colored charge transfer complex which will turn a yellow color upon the addition of a strong acid to the reaction mixture while the enzyme is reduced back to its native state. The blue colored complex shows an absorbance at 652 nm, whereas the yellow product shows an absorbance at 450 nm. These chromogenic substrates can be used with the enzyme mimicking materials instead of the HRP enzyme, and the peroxidase assay can be performed.[23,24]

Here, we mainly focused on the development of a peroxidase mimicking bimetallic MOF, which can be used for the dual mode detection of H_2O_2. Zeolitic imidazolate framework-8 (ZIF-8), which has Zn as the central metal ion and 2-methyl imidazole as the organic ligand, was chosen as the peroxidase mimicking material in this work. But ZIF-8 alone cannot mimic the properties of the peroxidase enzyme. However, it is observed that ZIF-8 doped with Cu displays the peroxidase mimicking property.[10] Hence, the Cu-doped bimetallic ZIF-8 (Cu@ZIF-8) is used for dual mode detection of H_2O_2 both spectrophotometrically as well as electrochemically. In this work an attempt has been made to electrochemically sense H_2O_2 in the presence of the chromogenic substrate, which acts as a mediator, and Cu@ZIF-8, which acts as the peroxidase mimicking material, and this method exactly mimics the

https://doi.org/10.1021/acsomega.3c05535
ACS Omega 2023, 8, 39636−39650

colorimetric procedure. A chromogenic substrate, TMB, is successfully stabilized over the electrode surface, along with Cu@ZIF-8, and is utilized for electrochemical H_2O_2 sensing.[25] With the convincing results obtained from the above sensing strategies, the same is used for the detection of H_2O_2 in a raw milk sample.[21]

2. MATERIALS AND METHODS

2.1. Chemicals and Reagents. Copper nitrate trihydrate, zinc acetate dihydrate, 2-methylimidazole (99%, Sigma), 3,3′,5,5′-tetramethylbenzidine (TMB; ≥99%, Sigma), hydrogen peroxide (H_2O_2; 30% w/v, Sigma), Nafion (5% w/w in water and 1-propanol, Thermo Fischer), disodium hydrogen phosphate, sodium dihydrogen phosphate, cholesterol (≥99%, Sigma), melamine, urea, lactose, salicylic acid, sodium acetate, acetic acid, ethanol, and methanol are the chemicals used in this work. All of these chemicals and reagents were used as received without any further purification. Millipore water having a resistivity of 18.2 MΩ cm obtained from the Merck Millipore water system is used for the preparation of all of the aqueous solutions and for analytical purposes.

2.2. Methods. Previously reported synthesis strategies with slight modifications were utilized for the synthesis of both ZIF-8 as well as Cu@ZIF-8.[10] A detailed synthesis procedure is mentioned below.

2.2.1. Synthesis of ZIF-8. A water assisted synthesis method was adopted for the preparation of ZIF-8.[26] Zinc acetate (293 mg) and 2-methyl imidazole (1.08 g) were dissolved in 10 and 20 mL of Millipore water, respectively. Both these solutions were mixed together and stirred for 24 h. A white colored precipitate that formed was removed from the supernatant solution by centrifugation (7000 rpm, 15 min). The precipitate thus obtained was further washed with Millipore water and dried in air at 60 °C for 24 h.

2.2.2. Synthesis of Cu@ZIF-8. The white colored ZIF-8 powder prepared as above was used for the synthesis of Cu@ZIF-8.[10] Two different concentrations of copper nitrate hexahydrate solutions (0.03 mM and 1 mM) were prepared in ethanol solvent. To these solutions, 60 mg of previously prepared ZIF-8 powder was added, and the mixture was stirred for 1 h. The light blue colored precipitate thus obtained was washed thrice with methanol and dried in a vacuum at 60 °C for 24 h.

2.3. Spectrophotometric Detection of H_2O_2. The peroxidase mimicking activity of Cu@ZIF-8 was demonstrated spectrophotometrically using a peroxidase assay. TMB was used as the chromogenic substrate. About 100 μg of Cu@ZIF-8-1 (0.03 mM Cu loading) and Cu@ZIF-8-2 (1 mM Cu loading) were mixed with H_2O_2. The concentration of H_2O_2 was varied from 1 mM to 50 mM. To this mixture, 1 M sodium acetate buffer (pH 3.8) was added along with freshly prepared TMB solution (1 mM) in DMSO. The total reaction volume was maintained at 1 mL. The blue colored assay mixture was incubated for 15 min, and UV−visible spectra were recorded at 660 nm to measure the corresponding absorbance values.

Similarly, TMB concentration was also varied from 0.1 mM to 0.9 mM with a fixed concentration of H_2O_2 (1 M) and 100 μg of either Cu@ZIF-8-1 or Cu@ZIF-8-2 in a separate experiment. The blue colored assay mixture was incubated for 15 min, and UV−visible spectra were recorded at 660 nm to determine the corresponding absorbance values.

2.3.1. Enzyme Kinetic Studies. The peroxidase mimetic activity of Cu@ZIF-8 was analyzed, based on the Michaelis−Menten equation. For this purpose, UV−visible absorption spectroscopic studies were carried out in the time scan mode, and a plot of absorbance (measured @660 nm) vs time was obtained. This experiment was carried out over various concentration ranges of H_2O_2 (1 mM to 50 mM) and TMB (0.1 mM to 0.9 mM). Using the initial rate method, first the catalytic reaction velocity was obtained and was used to get the typical Michaelis−Menten curve by plotting catalytic reaction velocity (V) against the concentration of the substrate. From the Michaelis−Menten curve, a Lineweaver−Burk double reciprocal plot was obtained by plotting $1/V$ vs $1/[S]$ where S is the substrate. From the slope and intercept values of this plot, kinetic parameters like the Michaelis−Menten constant (K_m) and maximum rate of the substrate conversion (V_{max}) were determined.

2.4. Electrochemical Detection of H_2O_2. The peroxidase mimicking behavior of Cu@ZIF-8 was also investigated using electrochemical methods as well. All of the electrochemical studies were carried out using a typical three electrode system with a glassy carbon electrode (GCE; Φ = 3 mm) as a working electrode, Pt wire as a counter electrode, and Ag/AgCl as a reference electrode, respectively. A well-polished GCE was modified with 2.5 μL of Cu@ZIF-8 (1 mg/0.5 mL ethanol) and allowed to dry overnight (Cu@ZIF-8/GCE). Cyclic voltametric (CV) studies were carried out in a potential range of 0.6 V to −0.65 V, and correspondingly the amperometric studies were carried out at an applied potential of −0.25 V using the modified electrode for various concentrations of H_2O_2 in PBS (pH 7) under N_2 purged conditions.

Similarly, the effect of TMB on the electrochemical peroxide detection was also investigated. For this purpose, a mixture of TMB (1 mg/mL in DMSO) and Nafion (0.5 wt %; 1:1) solution was prepared, and 2.5 μL of this solution was drop-cast over a well-polished GCE (TMB/Nf/GCE). The modified electrode was used to study TMB electrochemistry by cyclic voltammetry in a potential range of −0.4 to 0.8 V in an acetate buffer (pH 5) and PBS (pH 7) under N_2 purged conditions. To study the peroxide sensing, TMB/Nf/GCE was further modified with 2.5 μL of Cu@ZIF-8 and dried overnight (Cu@ZIF-8/TMB/Nf/GCE). Thus, the modified electrode was used for CV studies in a potential range of 0.8 V to −0.4 V in an acetate buffer as well as PBS and the amperometric studies at an applied potential of 0.1 V in acetate buffer and −0.1 V in PBS. All of the experiments were carried out under N_2 purged conditions.

2.5. Interference Studies and Real Sample Analysis. Interference studies were carried out using spectrophotometric and electrochemical methods. Cholesterol, melamine, urea, salicylic acid, and lactose at a concentration level of 1 mM were chosen as the interferents in order to evaluate the selectivity of the proposed biosensor. Further, milk was chosen for real time sensing of peroxide.[21,27−29] Raw milk from a local shop was purchased and spiked with definite concentrations of H_2O_2. A real sample analysis was carried out using UV−visible spectroscopic and electrochemical methods. The experiments with the real samples were carried out in sodium acetate buffer under N_2 purged conditions. Milk samples were spiked with specific concentrations of H_2O_2 ranging from 1 mM to 10 mM, and the recovery percentage of the analyte, H_2O_2, was also calculated.

https://doi.org/10.1021/acsomega.3c05535
ACS Omega 2023, 8, 39636−39650

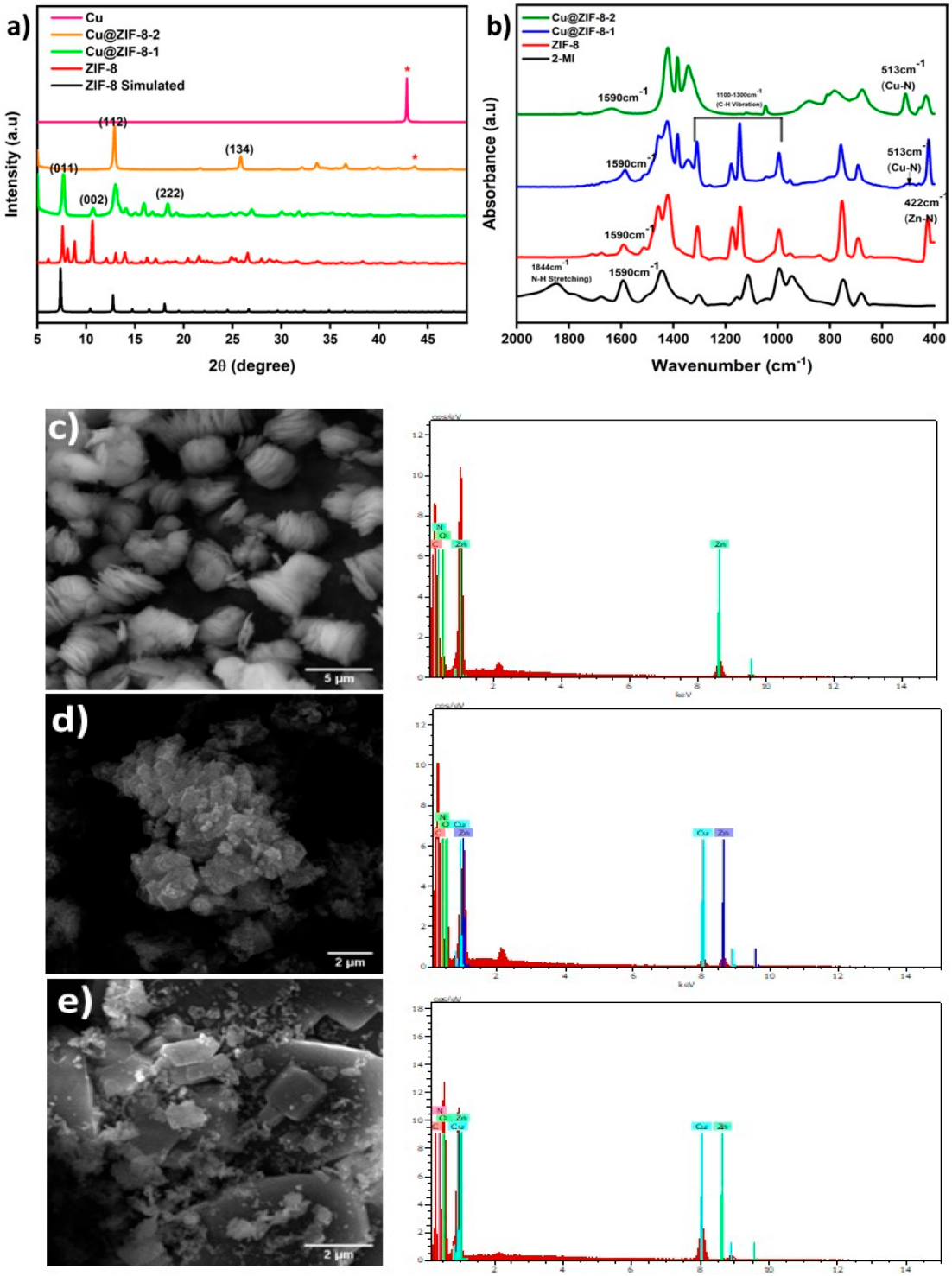

Figure 1. (a) XRD pattern of ZIF-8 and Cu@ZIF-8. (b) FTIR spectra of ZIF-8 and Cu@ZIF-8. SEM images and the corresponding EDS data of (c) ZIF-8, (d) Cu@ZIF-8-1, and (e) Cu@ZIF-8-2, respectively.

3. RESULTS AND DISCUSSION

3.1. Characterization of Cu@ZIF-8. The crystalline structure and phase purity of ZIF-8 as well as Cu@ZIF-8 were studied by analyzing XRD patterns (Figure 1a). ZIF-8 is characterized by its typical crystal planes of (011), (002), (222), and (134). The minor changes observed between the XRD patterns of the simulated and experimental XRD are due to changes in the method of preparation like variation of the solvent, temperature, and molar ratio between the metal Zn and the ligand 2-methyl imidazole. The influence of changes in the experimental methodologies affect the morphology and the crystalline nature of the sample, which was well exemplified by Jian et al. for the water-based synthesis of ZIF-8 at high morphology levels.[26] The sharp peaks in XRD represent the highly crystalline nature of the materials. Once ZIF-8 was doped with copper (Cu@ZIF-8-1), it still retained the characteristic peaks of ZIF-8. As the concentration of copper

https://doi.org/10.1021/acsomega.3c05535
ACS Omega 2023, 8, 39636−39650

was further increased (Cu@ZIF-8-2, 1 mM Cu), the (011) facet disappeared in the XRD pattern. This indicates that, as the copper concentration increased, the coordination between zinc and 2-methyl imidazole was broken and further copper was coordinated to the ligand. This suggests the etching of certain facets of ZIF-8 by copper ions. Further, the presence of copper can also be confirmed, as the XRD pattern matches well with the typical XRD pattern of copper. In the case of Cu@ZIF-8-2, a peak is noted at 43.71° which matches with the copper peak at 42.87°. But this peak is not visible in the case of Cu@ZIF-8-1, due to the very low concentration of copper.

FTIR studies were carried out to confirm the bonding between copper and the ligand (Figure 1b). The bonding between Zn and nitrogen is confirmed by the sharp peak appearing at 422 cm^{-1}, which is present in both ZIF-8 as well as Cu@ZIF-8. The appearance of a prominent peak at 513 cm^{-1} indicates the bonding between Cu and N, which is clearly absent in the case of ZIF-8. This peak confirms that the added copper is bonded to the ligand. Similarly, the peak observed at 1844 cm^{-1} indicates the N−H stretching frequency arising from 2-methyl imidazole. This peak is absent in the case of ZIF-8 and Cu@ZIF-8, which indicates the bonding between the metal center and the ligand.

Morphological features were analyzed using microscopic analysis. SEM images of ZIF-8 as well as Cu@ZIF-8 and their corresponding energy dispersive X-ray spectra (EDS) are shown in Figure 1c−e. Since water is used as a solvent for ZIF-8 synthesis, a multilayered 2D structure with stacked hexagonal sheets was obtained instead of the typical truncated rhombic dodecahedron. This multilayered structure was disrupted upon the addition of copper ions as it causes the etching of the hexagonal sheets. EDS analysis proves the presence of copper, zinc, and nitrogen present in Cu@ZIF-8-1 and Cu@ZIF-8-2.

In order to analyze the elemental composition and oxidation states of the elements present in the peroxidase mimicking material, X-ray photoelectron spectroscopy (XPS) was performed.[30] The full scan survey spectrum confirmed the presence of Zn, N, O, and C in the case of ZIF-8 and additionally Cu in Cu@ZIF-8 materials. A survey (Figure S1; Supporting Information [SI]) spectrum shows that the atomic percentage of Zn has reduced correspondingly with the concomitant enhancement in Cu concentration (Table 1).

Table 1. Comparison of Atomic Percentage of Zn, Cu, and N in Cu@ZIF-8-1 and Cu@ZIF-8-2

sample	element	atomic %
ZIF-8	Zn	8.63
	N	25.34
Cu@ZIF-8-1	Cu	8.26
	Zn	8.54
	N	16.65
Cu@ZIF-8-2	Cu	14.32
	Zn	1.09
	N	9.81

For Cu@ZIF-8-1, there are two Zn 2p peaks, viz, Zn $2p_{1/2}$ and Zn $2p_{3/2}$ at 1043.4 and 1020.45 eV, respectively (Figure 2a), and these peaks are slightly shifted to more positive binding energy in the case of Cu@ZIF-8-2 (Figure 2b). These two peaks correspond to the presence of a Zn^{2+} state. In the case of copper, too, two Cu 2p peaks, viz, Cu $2p_{1/2}$ and Cu $2p_{3/2}$, are observed along with two satellite peaks, which indicates its +2 oxidation state in both Cu@ZIF-8-1 and Cu@ZIF-8-2 samples (Figure 2b). There are three major peaks for N 1s, namely, pyridinic nitrogen, pyrrolic nitrogen, and N=C. The spectrum indicates that the metal ions are coordinated to the pyrrolic N, and as the concentration of copper increases, the pyridinic nitrogen and pyrrolic nitrogen peaks are distorted, which confirms the coordination of metal center with N.

3.2. Peroxidase Mimetic Activity of Cu@ZIF-8. The peroxidase mimicking property of Cu@ZIF-8 is demonstrated using a simple peroxidase assay.[31] In a basic peroxidase assay, HRP enzyme will be oxidized by H_2O_2. This oxidized HRP in turn will remove one electron from TMB, which will form two intermediate oxidation state products. This consists of a colorless TMB cation radical that is in rapid chemical equilibrium with a second blue-green colored intermediate oxidation state entity (charge transfer complex, CTC). This CTC shows an absorbance peak at 652 nm in the UV−visible spectrum. Once the enzyme oxidizes TMB, it will return back to its native state (Scheme 1).[32,33] In a similar way, Cu@ZIF-8, which exhibits peroxidase mimicking properties, can be used for TMB oxidation, and thus its enzymatic kinetics can be studied spectrophotometrically (Scheme 1). This peroxidase mimicking property can be utilized for H_2O_2 detection.

The enzyme kinetic parameters are usually calculated based on the Michaelis−Menten equation. Consider the enzyme catalytic reaction (eq 1):

$$E + S \underset{k_1}{\overset{k_{-1}}{\rightleftharpoons}} [ES] \overset{K_2}{\rightarrow} P + E \quad (1)$$

where E is the enzyme, S is the substrate, and P is the product. Here, the enzyme (E) is replaced by enzyme mimicking material Cu@ZIF-8. TMB and H_2O_2 are the substrates. The Michaelis−Menten equation for this system can be represented as (eq 2):

$$V = \frac{V_{max}[S]}{K_m + [S]} \quad (2)$$

where V is the rate of substrate conversion, V_{max} is maximum rate of substrate conversion, [S] is the concentration of the substrate, and K_m is the Michaelis−Menten constant. Thus, to study the kinetic parameters of the enzyme mimic, Cu@ZIF-8, Michaelis−Menten kinetics was utilized.

Initially, the peroxidase assay was carried out with ZIF-8 along with a mixture of TMB and H_2O_2 in an acetate buffer. Interestingly, ZIF-8 did not produce any blue color, which indicates its inability to act as a peroxidase mimic. The comparison of E° values of the reagents is given in the Supporting Information (Table S1). Afterward, the peroxidase assay was repeated with copper modified ZIF-8 (Cu@ZIF-8) along with a mixture of TMB and H_2O_2 in acetate buffer, which produces a visible blue colored solution. This indicates that ZIF-8 alone cannot act as a peroxidase mimic, but when doped with copper it shows peroxidase like behavior (Figure 3a). The peroxidase enzyme mimicking reaction occurs at the cuprous/cupric redox center of Cu@ZIF-8. Initially, Cu^+ formation is facilitated by a Fenton like reaction as shown below (eq 3).[14] Cu^+ centers are responsible for the reduction of H_2O_2 (eq 4), and Cu^+ centers are in turn oxidized to Cu^{2+}, which then oxidizes TMB to TMB^+ and reduces back to Cu^+ ions (eq 5; Scheme 1).

https://doi.org/10.1021/acsomega.3c05535
ACS Omega 2023, 8, 39636−39650

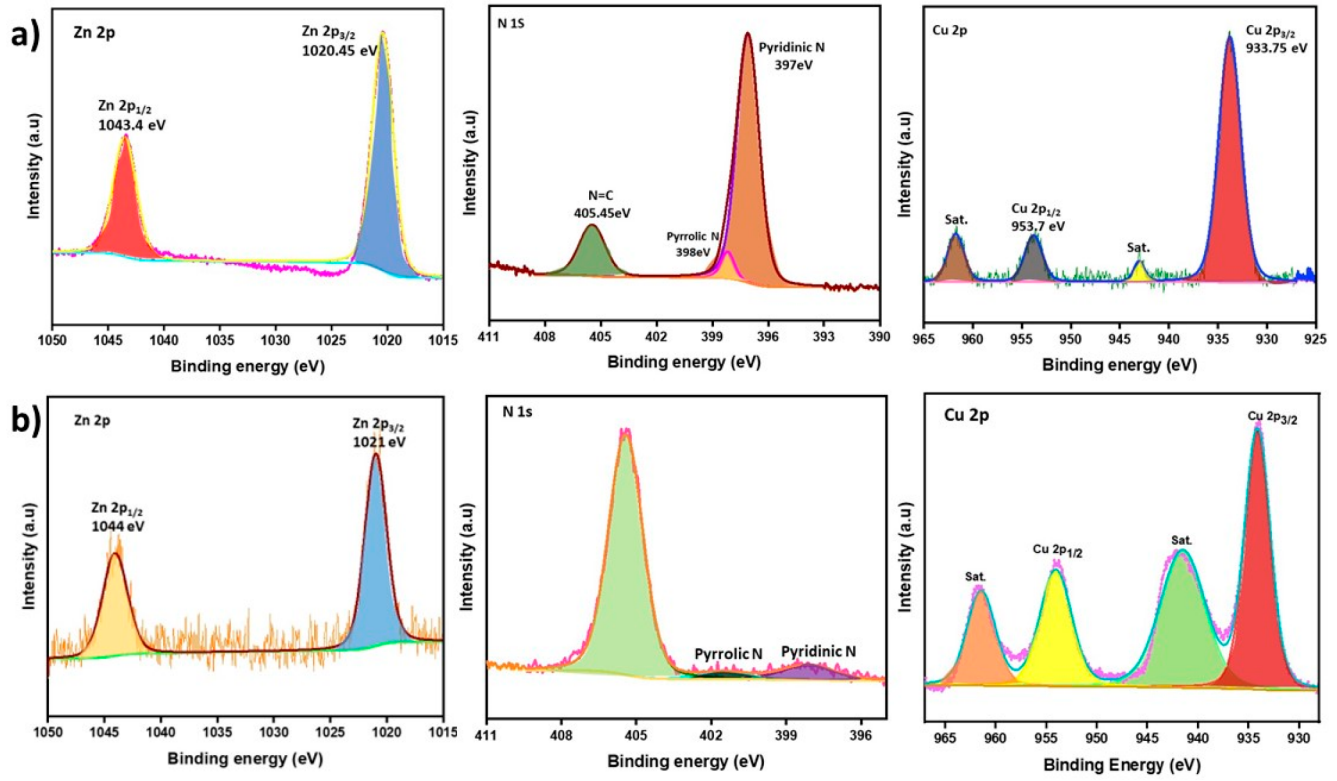

Figure 2. XPS spectra of (a) Cu@ZIF-8-1 and (b) Cu@ZIF-8-2.

Scheme 1. Pictorial Illustration of TMB Oxidation by HRP Enzyme and the Enzyme Mimic, Cu@ZIF-8

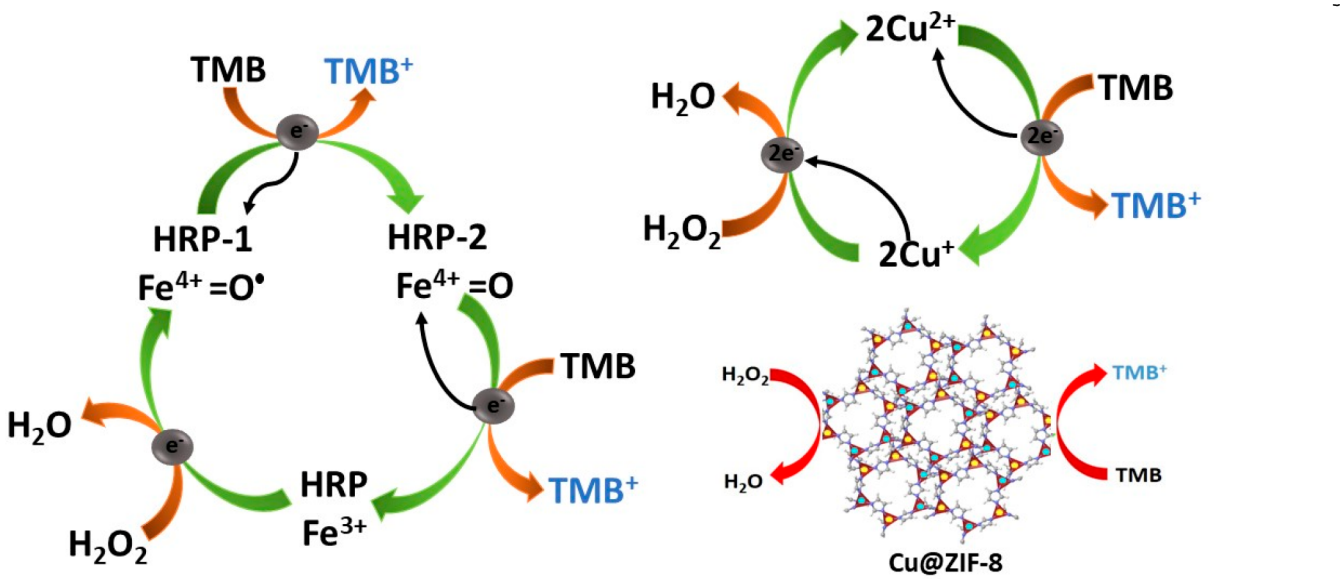

$$2Cu^{2+} \rightarrow 2Cu^{+} + 2e^{-} \text{ (Fenton-like reaction in presence of } H_2O_2) \quad (3)$$

$$2Cu^{+} + H_2O_2 \rightarrow 2Cu^{2+} + H_2O \quad (4)$$

$$TMB + Cu^{2+} \rightarrow TMB^{+} + Cu^{+} \quad (5)$$

Zinc ions however cannot exchange electrons with TMB to form a blue colored oxidized product because of the inherent E° value. Thus, it is evident that Zn does not play any role in the enzyme mimic.

Also, it is observed that, in the absence of H_2O_2, Cu@ZIF-8 does not produce any blue color, which indicates that the peroxidase mimic does not directly oxidize TMB. Maximum absorbance intensity was observed at a 660 nm wavelength. The absorbance peak noticed at 660 nm is attributed to the oxidation of TMB to TMB^{+} by Cu@ZIF-8 in the presence of H_2O_2. Since the peroxidase assay is highly dependent on the pH of the reaction mixture, the optimum pH for the reaction was determined by varying the pH of the sodium acetate buffer from 3.82 to 5.44. It was found that the maximum peroxidase-

https://doi.org/10.1021/acsomega.3c05535
ACS Omega 2023, 8, 39636−39650

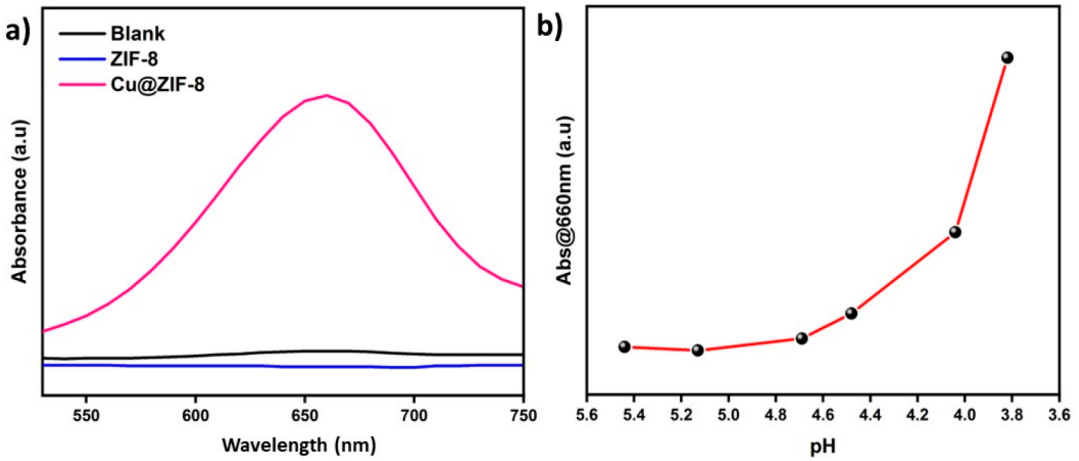

Figure 3. (a) UV−visible spectra of TMB oxidation recorded using the peroxidase mimic Cu@ZIF-8 in the presence of H_2O_2 and TMB in an acetate buffer (pH 3.82; pink), Cu@ZIF-8 and TMB in the absence of H_2O_2 in an acetate buffer (pH 3.82; black), and ZIF-8 and TMB in the presence of H_2O_2 in an acetate buffer (pH 3.82; blue). (b) A plot of absorbance intensity vs pH for TMB oxidation recorded at different pH values of acetate buffer.

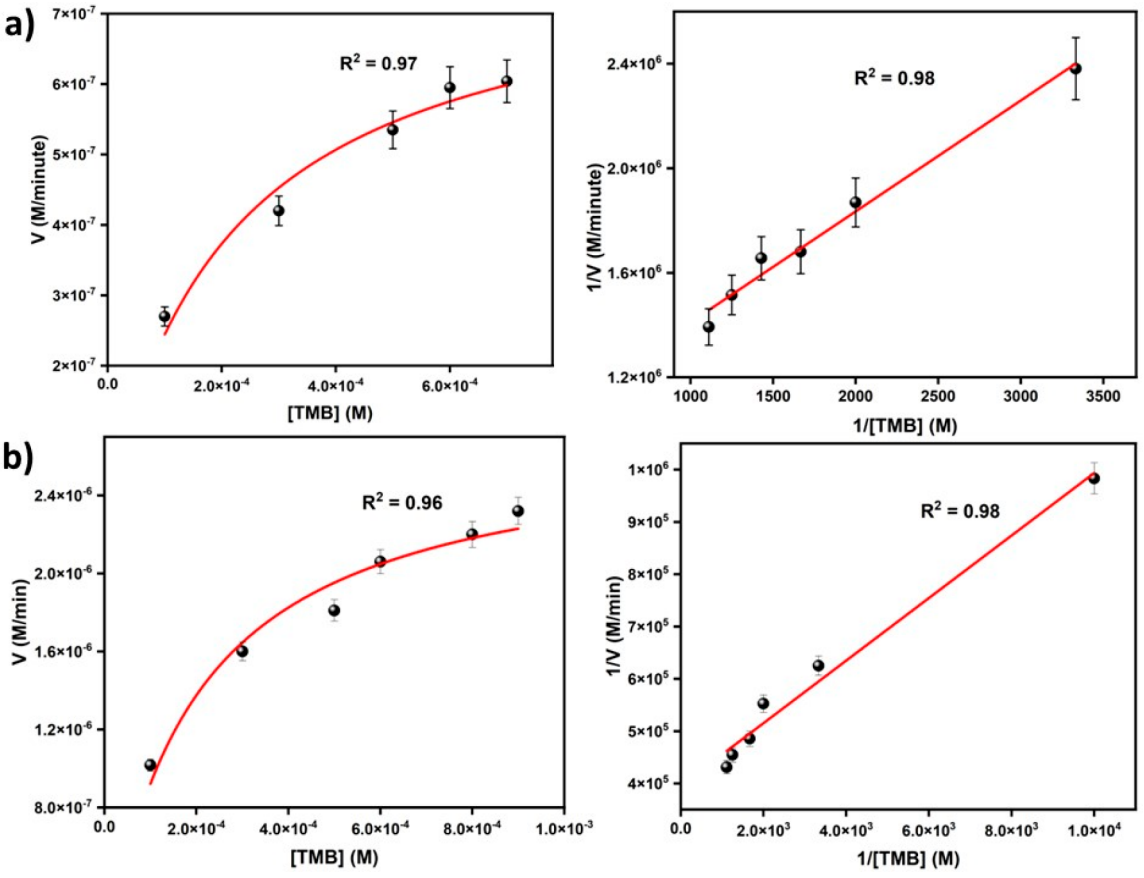

Figure 4. Michaelis−Menten curves for different concentrations of TMB at a constant concentration of H_2O_2 (1 M) in acetate buffer (pH 3.82) and the corresponding Lineweaver−Burk plots for (a) Cu@ZIF-8-1 and (b) Cu@ZIF-8-2.

like activity was obtained at a pH of 3.82, and it was chosen as the optimum pH for further studies (Figure 3b).

Steady state kinetic parameters of the peroxidase mimic were determined by varying the concentrations of H_2O_2 and TMB. The concentration of H_2O_2 was varied from 1 mM to 50 mM at a constant concentration of 1 mM TMB. The TMB concentration was varied from 0.1 mM to 0.9 mM by keeping H_2O_2 concentration constant at 1 M. The total reaction volume for both the reactions was made up to 1 mL by using a sodium acetate buffer at a pH of 3.82. The experiment was carried out with ZIF-8 doped by two different concentrations of Cu. i.e., 0.03 mM and 1 mM. Variations in the absorbance values with time were measured at a fixed wavelength of 660 nm (Figure S2). Kinetic parameters were determined using the initial rate method. Concentrations of H_2O_2 as well as TMB were obtained from the time scan data (Figure S2) by applying

https://doi.org/10.1021/acsomega.3c05535
ACS Omega 2023, 8, 39636−39650

the Beer–Lamberts law, in which the molar absorption coefficient of oxidized TMB is taken as ε = 39 000 M^{-1} cm^{-1}.[34] This concentration term corresponds to the velocity of the reaction (V), and a plot between V and concentration of the substrate will provide the corresponding Michaelis–Menten curves. By taking the reciprocal of the parameters V and the concentration of substrates, Michaelis–Menten curves were converted into the corresponding Lineweaver–Burk double reciprocal plots (eq 6).

$$\frac{1}{V} = \frac{K_m}{V_{max}}\frac{1}{[S]} + \frac{1}{V_{max}} \quad (6)$$

Kinetic parameters K_m and V_{max} were calculated from the Lineweaver–Burk plot. The Michaelis–Menten constant (K_m) indicates the affinity of an enzyme toward the substrate. A smaller K_m value reflects the stronger affinity of an enzyme toward the substrate. V_{max} is the maximum velocity at which all of the enzyme active sites are saturated with the substrate, and it is directly proportional to the concentration of the enzyme.

Initially, to obtain the kinetic parameters, H_2O_2 was used as the substrate, and its concentration was varied from 1 mM to 50 mM by keeping the TMB concentration constant. The assay was performed for both Cu@ZIF-8-1 and Cu@ZIF-8-2. A typical Michaelis–Menten curve was obtained for both Cu@ZIF-8-1 (Figure S3a) and Cu@ZIF-8-2 (Figure S3b). A corresponding Lineweaver–Burk plot was also obtained from the Michaelis–Menten curve (Figure S3). For Cu@ZIF-8-1, the apparent K_m and V_{max} values are determined to be 6.7 × 10^{-3} M and 0.9 × 10^{-8} M/s, respectively. Further, in the case of Cu@ZIF-8-2, the K_m and V_{max} values are calculated to be 8.93 × 10^{-3} M and 3.02 × 10^{-8} M/s, respectively.

For further analysis of kinetic parameters, TMB was used as the substrate, and its concentration was varied from 0.1 mM to 0.9 mM, by keeping the H_2O_2 concentration constant. The assay was performed for both Cu@ZIF-8-1 and Cu@ZIF-8-2. A typical Michaelis–Menten curve was obtained for both Cu@ZIF-8-1 (Figure 4a) and Cu@ZIF-8-2 (Figure 4b). The corresponding Lineweaver–Burk plots were also obtained from the Michaelis–Menten curves. For Cu@ZIF-8-1, the apparent K_m and V_{max} values are obtained as 0.22 × 10^{-3} M and 1.31 × 10^{-8} M/s. Moreover, for the case of Cu@ZIF-8-2, the K_m and V_{max} values are calculated to be 0.19 × 10^{-3} M and 4.51 × 10^{-8} M/s, respectively.

The determined K_m and V_{max} values indicate that both Cu@ZIF-8-1 and Cu@ZIF-8-2 have smaller K_m values with TMB as the substrate than HRP, which reflects upon the higher affinity of the enzyme mimics toward TMB when compared to the natural enzyme, HRP. But in the case of H_2O_2 as a substrate, K_m values are higher compared to HRP, which indicates their lesser affinity toward H_2O_2 than the enzyme, HRP. Hence, both Cu@ZIF-8-1 and Cu@ZIF-8-2 functioning as enzyme mimics can bind with the TMB substrate effectively, and thus efficient TMB oxidation will take place, which is useful for the peroxidase assay. Also, the V_{max} value of Cu@ZIF-8-2 is higher than that of Cu@ZIF-8-1. This is due to the higher concentration of copper in Cu@ZIF-8-2 than Cu@ZIF-8-1. Thus, the increasing concentration of copper leads to the enhancement in the velocity of peroxidase assay. A comparison of K_m and V_{max} values of Cu@ZIF-8 with other Cu-based MOFs and natural enzyme HRP is given in Table 2.

3.2.1. Selectivity Studies. Selectivity studies are necessary to prove the applicability of a sensor for real sample analysis and practical applications. Thus, to ensure the specificity of the enzyme mimic, selectivity studies were carried out using a colorimetric method. Some possible interferences that may be present in the milk sample were selected and analyzed. This includes cholesterol, lactose, urea, salicylic acid, and melamine. Selectivity studies were carried out using the same procedure followed for the peroxidase analysis. Our studies clearly prove that none of these interferences produce any visible color and did not show the corresponding absorbance peak at 660 nm during the peroxidase assay (Figure S4), which indicates the specificity of the Cu@ZIF-8 enzyme mimic.

Table 2. Comparison of K_m and V_{max} Values of Cu@ZIF-8 with Other Cu-Based MOFs As Well As the Natural Enzyme HRP

mimic material	substrate	K_m (M; 10^{-3})	V_{max} (M/s; 10^{-8})
Cu@ZIF-8-1[a]	TMB	0.22	1.31
	H_2O_2	6.7	0.91
Cu@ZIF-8-2[a]	TMB	0.19	4.51
	H_2O_2	8.93	3.02
HRP[23]	TMB	0.43	10
	H_2O_2	3.72	8.71
Cu-hemin MOF[6]	TMB	1.42	26.22
	H_2O_2	2.18	116
Cu-TCPP(Fe)[35]	TMB	0.05	8.61
	H_2O_2	26.7	16.26
$[Cu_2(L)_2]\cdot 2DMA\cdot 3H_2O$ (MOF)[36]	TMB	2.48	7.52
	H_2O_2	0.16	6.74

[a]This work.

3.2.2. Real Sample Analysis. In this work, a milk sample was used to study the real time applicability of Cu@ZIF-8 as a peroxidase mimic. The milk sample was obtained from the local stores in Karaikudi, Tamil Nadu, India. Recovery experiments were carried out using colorimetry by spiking the milk samples with specific concentrations of H_2O_2. The concentration of H_2O_2 was varied from 1 mM to 20 mM in the milk sample. A peroxidase assay was performed with these samples, and the obtained results are shown in Figure S5.

Initially ZIF-8, which lacks the peroxidase mimicking behavior, is converted into a peroxidase mimic by incorporating Cu ions into it. Using this Cu incorporated ZIF-8, peroxide sensing was carried out by colorimetric studies, and the corresponding kinetic parameters were determined. It was found that, as the amount of Cu ions incorporated in the MOF increases, the maximum catalytic velocity is enhanced. From the K_m value, it was found that the material possesses more affinity toward the TMB substrate. Also, the material is highly selective toward peroxide, and hence it is able to sense the presence of peroxide in milk samples.

3.3. Electrochemical Analysis of Enzyme Mimetic Activity of Cu@ZIF-8. *3.3.1. Electrochemical Peroxide Detection Using Cu@ZIF-8/GCE.* Initially, GCE modified with Cu@ZIF-8 was used to study the electrochemical sensing of peroxide in PBS (pH 7) under N_2 purged conditions. Cyclic voltametric (CV) studies were carried out in the potential range from 0.6 V to −0.65 V, and the concentration effect of H_2O_2 on Cu@ZIF-8/GCE was studied by varying the concentration from 0.5 mM to 3.5 mM (Figure 5a). A linear increase in reduction current is observed with increasing peroxide concentration, which is indicated by the calibration plot drawn between current and concentration of H_2O_2

https://doi.org/10.1021/acsomega.3c05535
ACS Omega 2023, 8, 39636−39650

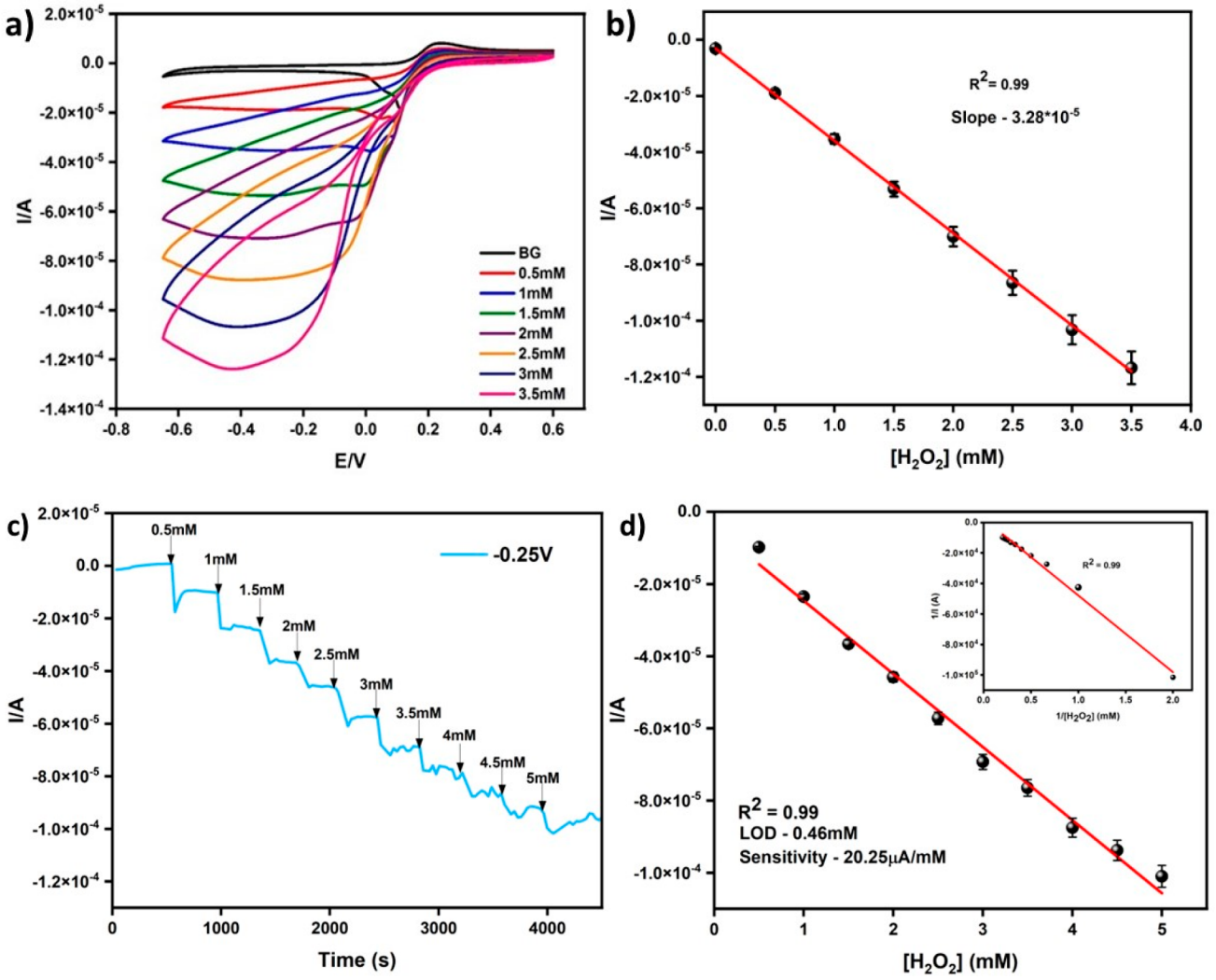

Figure 5. (a) Cyclic voltammograms recorded at a scan rate of 30 mV/s using GCE modified with Cu@ZIF-8-2 during the addition of increasing H_2O_2 concentrations. (b) Calibration curve between the current and the concentration of H_2O_2 using the data obtained from a. (c) Chronoamperometric study of GCE modified with Cu@ZIF-8-2 upon the addition of increasing H_2O_2 concentrations at an applied potential of −0.25 V. (d) Calibration curve obtained between the current and concentration of H_2O_2 from c. Inset shows the plot between the reciprocal of the current and concentration of H_2O_2, which is the electrochemical version of the Lineweaver−Burk plot. All of the experiments were carried out in PBS buffer (pH 7) under N_2 purged conditions.

(Figure 5b). Upon increasing the H_2O_2 concentration, the reduction peaks are observed to be broadened, and the peaks shifted to more negative reduction potential values. The increasing reduction current indicates the ability of Cu@ZIF-8 to catalytically reduce H_2O_2. A plot between log i_p vs log $[H_2O_2]$ generated a slope of 0.94 with a regression coefficient of 0.99, which indicates the first order kinetics of the reaction (Figure S6).

Chronoamperometric studies were carried out in order to study the effect of concentration variation at a fixed potential of −0.25 V for peroxide sensing. Studies were carried out in PBS (pH7) under N_2 purged conditions. The reduction current gradually increases with an increasing concentration of peroxide, and the calibration curve (I vs $[H_2O_2]$) exhibited a good linear response with an R^2 value of 0.99 between 0.5 mM and 5 mM (Figure 5c). Also, the rearrangement of the Michaelis−Menten equation (eq 7) will offer the electrochemical version of the Lineweaver−Burk plot (eq 8).

$$I = \frac{I_{max}[S]}{K_m^{app} + [S]} \tag{7}$$

$$\frac{1}{I} = \frac{1}{I_{max}} + \frac{K_m^{app}}{I_{max} \times [S]} \tag{8}$$

where I is the current, I_{max} is the maximum current under enzyme saturation conditions, K_m is the Michaelis−Menten constant, and S is the substrate concentration. The electrochemical version of the Lineweaver−Burk plot is obtained by plotting the reciprocal of the current and H_2O_2 concentration. Thus, a plot between the reciprocal of current and H_2O_2 concentration was drawn, and a linear plot with an R^2 value of 0.99 was obtained. From the slope of the curve, the Michaelis−Menten constant (K_m) was obtained as 0.0206 M. Also, it is observed that with an increase in concentration the variation in current is tending toward saturation. Thus, the peroxide sensing mechanism of Cu@ZIF-8 follows Michaelis−Menten kinetics electrochemically as well.

https://doi.org/10.1021/acsomega.3c05535
ACS Omega 2023, 8, 39636−39650

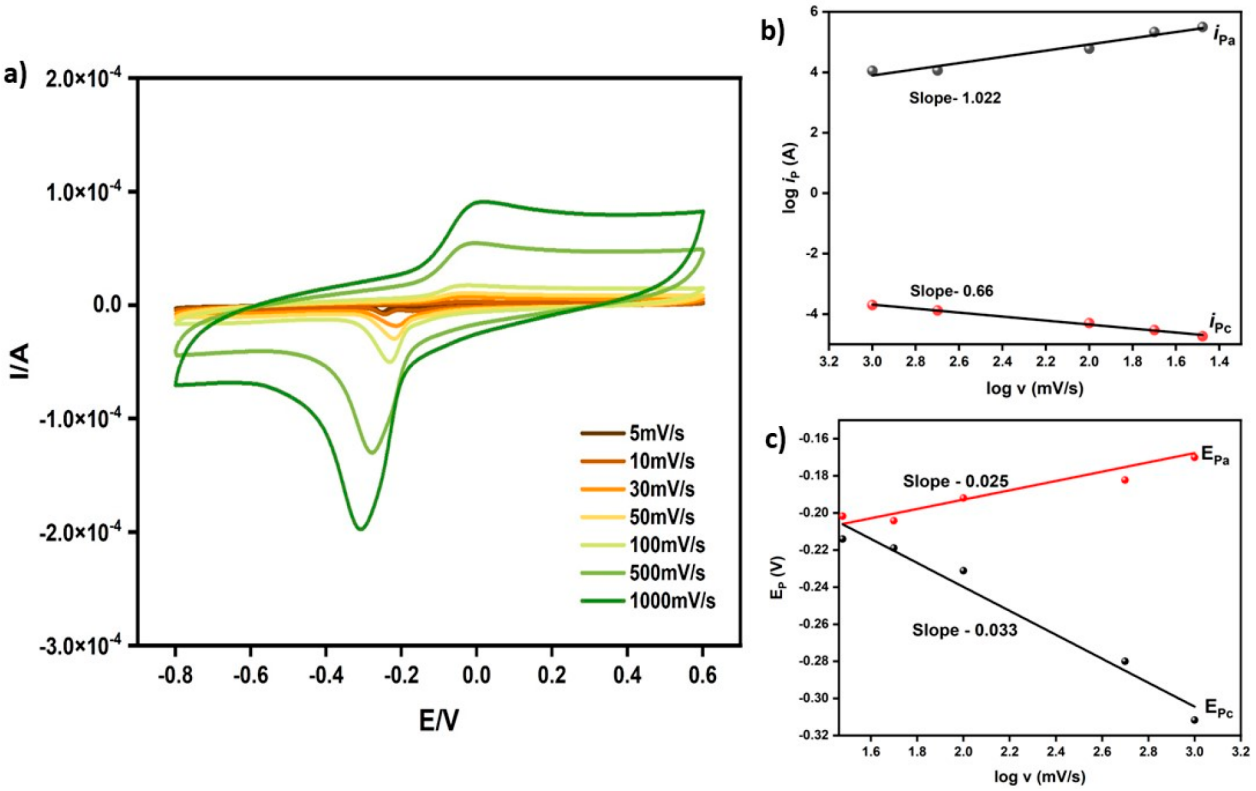

Figure 6. (a) Cyclic voltammograms recorded using GCE modified with Cu@ZIF-8-2 indicating the effect of scan rate. (b) Plot of log i_P vs log ν. (c) Plot of E_p vs log ν. All of the experiments were carried out in PBS (pH−7) under N_2 purged conditions.

The evaluation of chronoamperometric data helped in the determination of the limit of detection (LOD), sensitivity, and linear detection range of the proposed sensor. LOD was determined using the formula LOD = $3S/b$, where S is the standard deviation and b is the slope. The detection range was found to be 0.5 mM to 5 mM with an LOD of 0.46 mM at a working potential of −0.25 V. The sensitivity was found to be 20.25 μA/mM from the slope of the curve (Figure 5d).

3.3.2. Electrochemical behavior of Cu@ZIF-8/GCE. Further, to study the kinetics and mechanism of electrocatalytic peroxide reduction, scan rate studies were carried out using a Cu@ZIF-8-2/GC electrode in PBS (pH 7) under N_2 purged conditions by varying the scan rate from 5 to 1000 mV/s (Figure 6a).[37] We can observe a systematic increase in reduction current with increasing scan rate. The plot between log i_P (i_{Pa} and i_{Pc}) and log ν produced linear plots with slopes of 1.022 and 0.66, respectively (Figure 6b).

Charge transfer coefficient (α) and the apparent electron transfer rate constant (k_s) for a surface-controlled process was determined by applying Laviron theory.[38] For this purpose, an E_P (E_{Pa} and E_{Pc}) vs log ν plot was deduced, and corresponding slope values were determined to be 0.025 and 0.033 (Figure 6c). By applying these slope values in eq 9, the corresponding α value is determined.

$$\frac{S_a}{S_c} = \frac{\alpha}{1-\alpha} \tag{9}$$

Herem S_a and S_c are the slope values of linear plots E_{Pa} and E_{Pc} vs log ν, and α is the charge transfer coefficient. The α value is determined to be 0.431.

To determine the k_s value, eq 10 is used:

$$\log k_s = \alpha \log(1-\alpha) + (1-\alpha)\log\alpha - \log\frac{RT}{nF\nu} - \alpha(1-\alpha)n'F\frac{\Delta E_p}{RT} \tag{10}$$

where α is the charge transfer coefficient, n' is the number of electrons involved in the rate-determining step, ν is the applied scan rate, and ΔE_p is the peak separation, and this equation is applicable under the condition $n\Delta E_p > 200$ mV.

In order to determine the k_s value, the number of electrons involved in the rate-determining step (n') has to be determined initially. Thus, to determine the n' value theoretically, the previously determined α value is substituted in eq 11.[39]

$$\Delta E_{P_{1/2}} = \frac{62.5}{n'\alpha} \tag{11}$$

By assuming $n' = 1$, the $\Delta E_{P1/2}$ (full width at half-maximum, fwhm) value was obtained as 0.145 V. Now, from Figure 6a (scan rate analysis curve), the fwhm $\Delta E_{P1/2}$ values corresponding to each scan rate were determined. Thus, obtained $\Delta E_{P1/2}$ values at various scan rates were compared with the theoretical $\Delta E_{P1/2}$ value, and the values are found to be in agreement (Table 3). This indicates that the number of electrons involved in the rate-determining step is one, and thus Cu is reduced from a +2 to a +1 oxidation state during the redox reaction. By substituting α and n' values in eq 10, the corresponding k_s value is determined for higher scan rates alone as the equation is applicable for the condition $n\Delta E_p > 200$ mV. For 500 mV/s, the k_s value is 0.828 s^{-1}, whereas for 1000 mV/s, the k_s value is found to be 1.14 s^{-1}.

https://doi.org/10.1021/acsomega.3c05535
ACS Omega 2023, 8, 39636−39650

Table 3. Comparison of $\Delta E_{P1/2}$ and ΔE_P Values Measured at Various Scan Rates

scan rate (mV/s)	fwhm $\Delta E_{P1/2}$ (V)	ΔE_P (V)
30	0.112	0.173
50	0.095	0.175
100	0.098	0.191
500	0.163	0.258
1000	0.205	0.297

Thus, the probable mechanism of peroxide reduction by Cu@ZIF-8 proceeds as below:

(a) Electrode surface confined electron transfer:

$$2Cu^{2+} + 2e^- \rightarrow 2Cu^+ \quad (12)$$

(b) Electrocatalytic electron transfer with the reactant H_2O_2 in the solution:

$$2Cu^+ + H_2O_2 \rightarrow H_2O + 2Cu^{2+} \quad (13)$$

During the reductive scan (Figure 5a) of the CV, Cu ions in +2 oxidation in the MOF structure receive an electron from the electrode and get reduced to the Cu^+ state. This Cu^+ in turn will reduce H_2O_2 through a reaction probably involving a hydroxyl radical, and Cu^+ is converted back to the Cu^{2+} state. Thus, with an increasing concentration of H_2O_2, there will be a corresponding increase in the reduction current.

3.3.3. The Chromogenic Substrate, TMB, as an Electrochemical Mediator. Chromogenic substrate TMB is considered a good electrochemical redox mediator. Further, to exactly mimic the colorimetric peroxide sensing procedure and to study the effect of TMB on electrochemical peroxide sensing, GCE was modified with TMB (TMB/GCE), and its electrochemical characterization was performed. The existing literature reports discuss the electrochemical behavior of TMB in the solution phase.[23,40] But in this work, we have successfully immobilized TMB on GCE with good stability (Figure S7). The electrode surface was observed to have a bluish-green color, which can be considered an indication of TMB in the oxidized form. It is well-known that a two-electron transfer process is involved in TMB redox reactions.[41,42] TMB first gets oxidized to a blue-green-colored charge transfer complex (CTC) and further oxidized to a diamine product. To confirm this, CV studies were carried out in an acetate buffer at pH 5 and PBS at pH 7. As shown in Figure 7, we can observe two sets of oxidation and reduction peaks, which confirms the two-electron transfer process both in acetate buffer as well as PBS. In acetate buffer, during the anodic scan, TMB is oxidized to TMB^+ (0.408 V) and further oxidized to TMB^{2+} (0.698 V). Whereas in the cathodic scan, TMB^{2+} is reduced back to TMB^+ and TMB, which is indicated by the formation of peaks at 0.483 and 0.234 V. In PBS, during the anodic scan, TMB is oxidized to TMB^+ (0.427 V) and TMB^{2+} (0.684 V) in two steps, and in the cathodic scan TMB^{2+} is reduced back to TMB^+ (0.332 V) and further to TMB (0.156 V). In the case of PBS, the second oxidation step is particularly not well-defined.

The electrochemical behavior of TMB is highly pH dependent. The TMB redox reaction can either take place in two steps or in a single step, which is highly pH dependent. Therefore, pH variation (acetate buffer of pH 3.82 to 5 and PBS of pH 7) studies were carried out in order to optimize the pH suitable for sensor applications (Figure S8). Under highly acidic pH conditions, a single redox peak is observed which indicates that the TMB redox reaction takes place in a single step (Figure S8a). At pH 5.0, splitting of the redox peak is observed in the anodic and cathodic directions (Figure 7a). Also, in a PBS buffer of pH 7, two sets of redox peaks can be observed. (Figure 7b). Thus, at near neutral and neutral pH, the TMB redox reaction occurs in two steps, whereas in acidic pH the redox reaction follows a single step.

3.3.4. Electrochemical Peroxide Detection with Cu@ZIF-8/TMB/GCE. Electrochemical studies were carried out using Cu@ZIF-8/TMB/Nf/GCE in order to study the effect of TMB on peroxide sensing. These investigations were performed in both acetate buffer (pH 5) as well as PBS (pH 7) under N_2 purged conditions. Cyclic voltametric studies were carried out in a potential range of 0.8 V to −0.4 V with increasing concentrations of H_2O_2 (0.5 mM to 3.5 mM). Thus, with increasing H_2O_2 concentration, there is a corresponding increase in the reduction current both in acetate buffer as well as in PBS (Figure 8a,b). Interestingly, in the case of PBS,

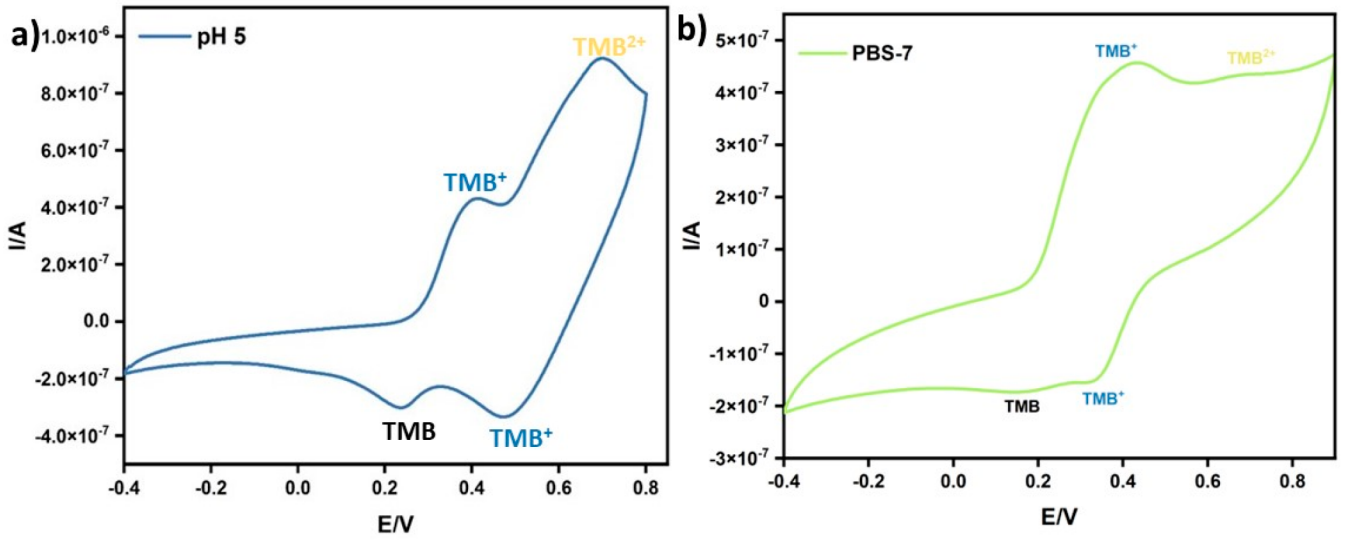

Figure 7. Cyclic voltammograms indicating a two-step TMB redox reaction in (a) acetate buffer (pH 5) and (b) PBS (pH 7) in a potential range of −0.4 to 0.8 V under N_2 purged conditions at a scan rate of 5 mV/s.

https://doi.org/10.1021/acsomega.3c05535
ACS Omega 2023, 8, 39636−39650

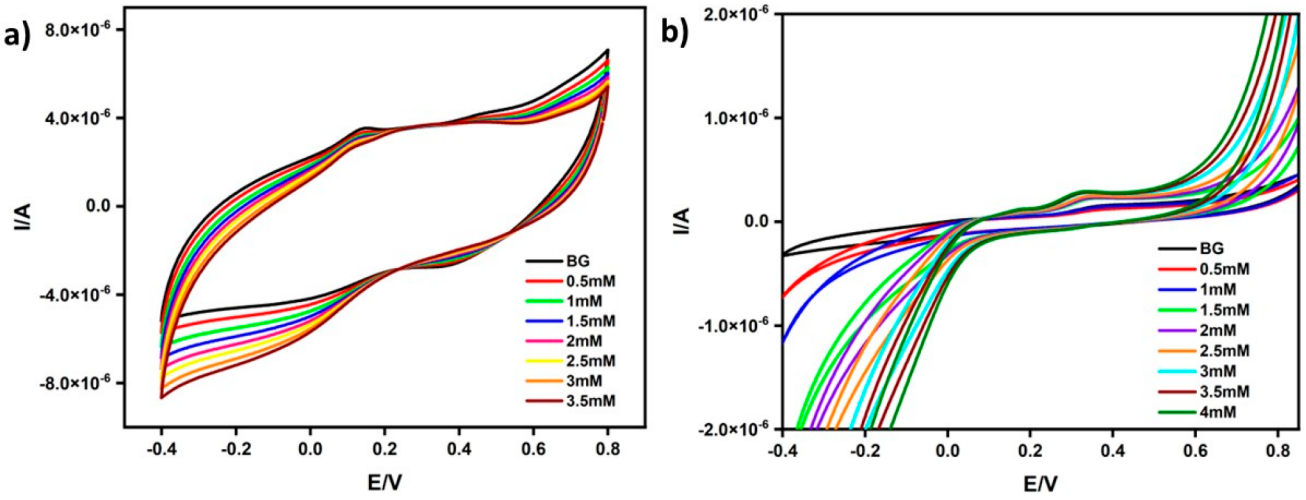

Figure 8. Cyclic voltammograms recorded using GCE modified with Cu@ZIF-8 and TMB under the addition of increasing H_2O_2 concentrations in (a) acetate buffer (pH 5) and (b) PBS (pH 7) under N_2 purged conditions in a potential range of 0.8 V to −0.4 V at a scan rate of 20 mV/s.

we can observe that the modified electrode can simultaneously catalyze the oxidation and reduction of H_2O_2 (Figure 8b). This can be advantageously used to catalytically sense H_2O_2 by either an electrooxidation or an electroreduction process.

The increase in reduction current with increasing H_2O_2 concentration can be explained as follows and is pictorially represented in Scheme 2: The chromogenic substrate, TMB, is in the oxidized TMB^+ state on the electrode surface. During the cathodic scan, the TMB^+ is reduced back to TMB (eq 14). This TMB will in turn react with Cu^{2+} in Cu@ZIF-8, and Cu^{2+} is reduced to Cu^+, whereas TMB is oxidized back to TMB^+ (eq 15). The Cu^+ will reduce H_2O_2 in the solution into hydroxyl radicals and is oxidized back to Cu^{2+} (eq 16). Thus, during the cathodic scan, the reduction current produced will increase correspondingly with increasing H_2O_2 concentration as TMB^+ and Cu^+ together can reduce more analyte, hydrogen peroxide.

Scheme 2. Pictorial Representation of Electrochemical Peroxide Sensing of Cu@ZIF-8: (a) in the Absence of TMB and (b) in the Presence of TMB

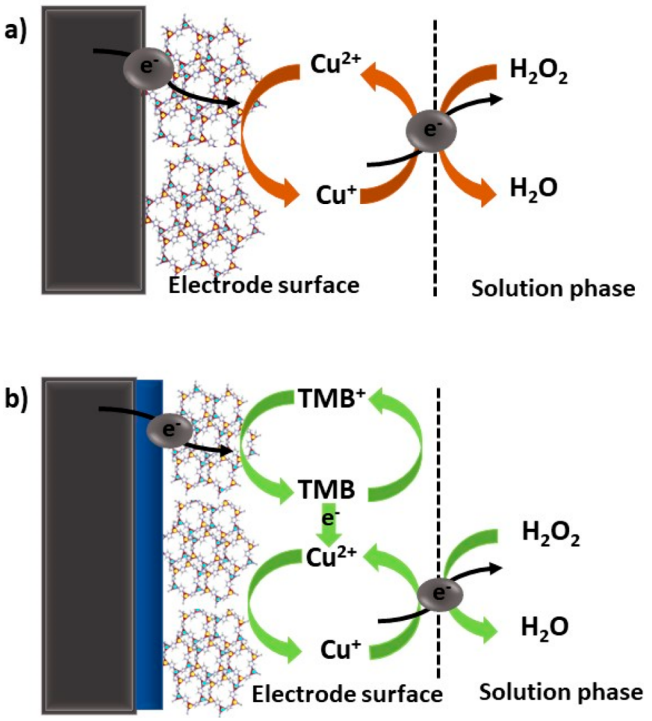

(a) Reaction on electrode surface

$$TMB^+ + e^- \rightarrow TMB \quad (14)$$

$$TMB + Cu^{2+} \rightarrow Cu^+ + TMB^+ \quad (15)$$

(b) Reaction in the solution:

$$2Cu^+ + H_2O_2 \rightarrow H_2O + 2Cu^{2+} \quad (16)$$

Further chronoamperometric studies were carried out in order to study the effect of TMB modification on peroxide sensing by Cu@ZIF-8 both in an acetate buffer (pH 5) and PBS (pH 7). We can observe that the peroxide reduction potential has shifted to a more positive reduction potential of 0.1 V when performed in acetate buffer and −0.1 V in PBS (pH 7). With each addition of H_2O_2 (0.5 mM), there is a corresponding increase in the reduction current (Figure 9a and c). The calibration curve plotted between current and concentration of H_2O_2 exhibits a good linear response (Figure 9b and d). LOD, sensitivity, and linear detection range values were calculated from the chronoamperometric data obtained at fixed potentials of 0.1 V and −0.1 V. Linear detection range was found to be between 0.5 mM and 5 mM with a LOD value of 0.4997 mM in acetate buffer and 0.143 mM in PBS. From the slope of the curve, the sensitivity of the sensor was found to be 0.097 μA/mM in acetate buffer and 0.33 μA/mM in PBS. A comparison of working potential, detection range, LOD, and sensitivity of the Cu@ZIF-8/GC and Cu@ZIF-8/TMB/GC electrodes is provided in Table 4. The inclusion of TMB as a mediator has decreased the working potential of amperometric detection of H_2O_2 by 0.35 V in acetate buffer and 0.15 V in phosphate buffer, which is a favorable outcome for the enzyme mimic materials.

3.3.5. Selectivity Studies. In order to develop an efficient sensor, its selectivity toward the specific analyte is highly important.[43] For this purpose, selectivity of our analytical method toward various interferents was evaluated. The effect of interferents on the electrochemical response of H_2O_2 was studied using the chronoamperometry technique using both

https://doi.org/10.1021/acsomega.3c05535
ACS Omega 2023, 8, 39636−39650

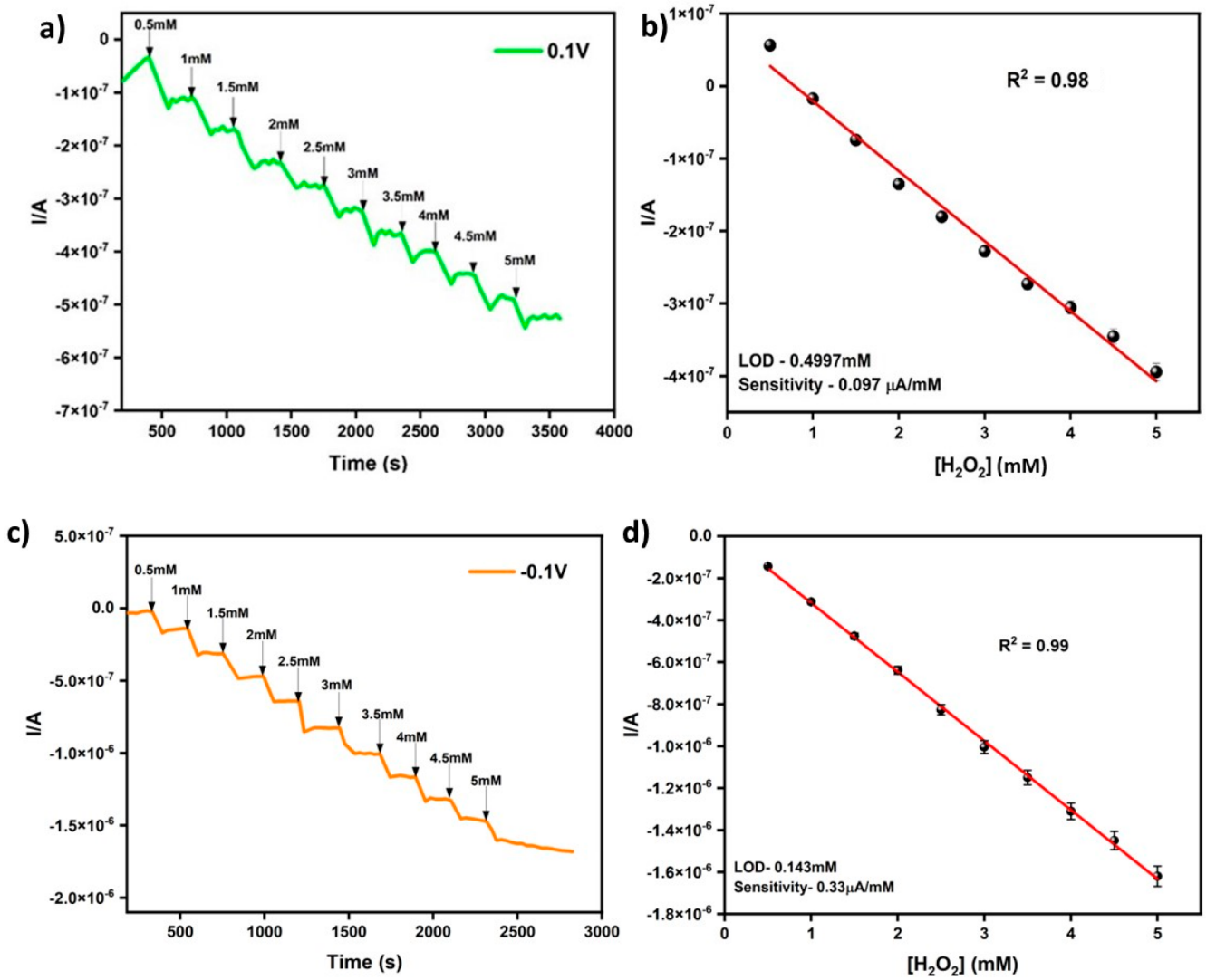

Figure 9. Chronoamperometric study of GCE modified with Cu@ZIF-8 and TMB during the addition of increasing H_2O_2 concentration in (a) acetate buffer at an applied potential of 0.1 V and (c) PBS at an applied potential of −0.1 V. b and d are the calibration curves drawn between current and H_2O_2 concentration.

Table 4. Comparison of Working Potential, Detection Range, LOD, and Sensitivity of Cu@ZIF-8/GCE and Cu@ ZIF-8/TMB/GCE

	Cu@ZIF-8/GCE	Cu@ZIF-8/TMB/GCE	
	PBS	acetate buffer	PBS
working potential	−0.25 V	0.1 V	−0.1 V
detection range	0.5 mM to 5 mM	0.5 mM to 5 mM	0.5 mM to 5 mM
LOD	0.46 mM	0.499 mM	0.143 mM
sensitivity	20.25 μA/mM	0.097 μA/mM	0.33 μA/mM

Cu@ZIF-8/GCE and Cu@ZIF-8/TMB/GCE modified electrodes. Cholesterol (1 mM), lactose (1 mM), salicylic acid (0.5 mm), urea (0.5 mM), and melamine (0.5 mM) were chosen as the potential interferents. The chronoamperometric studies were carried out in PBS (pH−7) at an applied potential of −0.25 V in the case of Cu@ZIF-8/GCE (Figure S9) and for Cu@ZIF-8/TMB/GCE in acetate buffer (pH 5) at an applied potential of 0.1 V (Figure S9). There is a rapid increase in current response upon the addition of 0.1 mM H_2O_2, whereas there is no obvious response on adding the interferents, which indicates the high selectivity of Cu@ZIF-8 toward the target analyte, peroxide.

3.3.6. Real Sample Analysis. A real sample analysis was carried out using milk samples obtained from the local store.[21] As stated earlier, peroxide is used as an antimicrobial agent which will prevent the spoilage of milk, and thus monitoring the presence of peroxide in milk samples is of high importance as it can cause serious health issues. Hence, chronoamperometric studies were carried out at a fixed potential of 0.1 V for Cu@ZIF-8/TMB/GCE in acetate buffer (pH 5) to determine the presence of peroxide in milk (Figure S10). The milk sample was used as such without any chemical treatment. Initially, raw milk samples were added, and we cannot observe any current response which indicates the absence of peroxide in milk. Further, the milk samples were spiked with specific concentrations of H_2O_2 and subjected to chronoamperometric studies. Upon the addition of milk samples spiked with peroxide, there is an obvious current response observed which indicates that Cu@ZIF-8 is able to trace out the presence of peroxide in milk. Thus, any milk samples adulterated with peroxide can be analyzed with the help of Cu@ZIF-8 as a

https://doi.org/10.1021/acsomega.3c05535
ACS Omega 2023, 8, 39636−39650

selective and sensitive peroxide sensor without any interference.

4. CONCLUSIONS

A Cu incorporated zeolitic imidazolate framework-8 (ZIF-8) is successfully synthesized, and the incorporation of Cu into ZIF-8 introduced a peroxidase mimicking behavior in ZIF-8. The ZIF-8 materials incorporating two different concentrations of Cu are synthesized and characterized. The peroxidase mimicking behavior of Cu@ZIF-8 is analyzed using spectrophotometric as well as electrochemical methods. The steady state kinetic parameters (K_m and V_{max}) of the material are determined spectrophotometrically, and it was found out that the material has more affinity toward the TMB substrate. Also, it was observed that, as the concentration of Cu in ZIF-8 increases, correspondingly the catalytic reaction velocity is also enhanced. The electrochemical characterization was carried out using two different systems, namely, Cu@ZIF-8/GCE and Cu@ZIF-8/TMB/GCE. Among the two, Cu@ZIF-8/GCE showed a LOD value of 0.46 mM with a sensitivity of 20.25 μA/mM at an applied potential of −0.25 V in PBS (pH 7), whereas Cu@ZIF-8/TMB/GCE exhibited a LOD value of 0.499 mM and 0.143 mM with a sensitivity of 0.097 μA/mM and 0.33 μA/mM at an applied potential of 0.1 V and −0.1 V in acetate buffer (pH 5) and PBS (pH 7), respectively. Here, we have demonstrated the successful immobilization of TMB on the electrode surface, and this modification has helped in shifting the applied working potential to a more positive value. Also, the sensing methodology is highly selective for H_2O_2, and the possibility of recovering peroxide from the milk samples using both electrochemical as well as spectrophotometric methods has been demonstrated. Thus, Cu@ZIF-8 is found to have good peroxidase mimicking behavior with good selectivity and sensitivity that suggest the material can be utilized for the dual mode detection of H_2O_2. Also, our further preliminary findings indicate the feasibility of extending this methodology for the detection of other bioanalytes like cholesterol, glucose, and lactate.

■ ASSOCIATED CONTENT

Supporting Information

The Supporting Information is available free of charge at https://pubs.acs.org/doi/10.1021/acsomega.3c05535.

XPS data comprising the survey scan spectra of Cu@ZIF-8-1 and Cu@ZIF-8-2, XPS spectrum of ZIF-8, enzyme kinetics data for TMB and H_2O_2, Michaelis−Menten and Lineweaver−Burk plots for varying concentrations of H_2O_2 studied using Cu@ZIF-8-1 and Cu@ZIF-8-2, selectivity studies for spectrophotometric detection of H_2O_2, spectrophotometric and amperometric studies corresponding to H_2O_2 spiked milk samples, log i_p vs log [H_2O_2] plot obtained from Figure 5a, electrochemical stability of TMB modified electrode, electrochemistry of TMB modified electrode at pH 3.8 and pH 4.69, interference studies carried out electrochemically with Cu@ZIF-8/GCE and Cu@ZIF-8/TMB/GCE, and a list of standard reduction potential values (PDF)

■ AUTHOR INFORMATION

Corresponding Authors

Sheela Berchmans − *Electrodics and Electrocatalysis (EEC) Division, CSIR—Central Electrochemical Research Institute (CSIR—CECRI), Karaikudi 630003 Tamil Nadu, India; Academy of Scientific and Industrial Research (AcSIR), Ghaziabad 201002, India;* orcid.org/0000-0003-4246-3348; Email: sheelaberchmans@yahoo.com

Ganesh Venkatachalam − *Electrodics and Electrocatalysis (EEC) Division, CSIR—Central Electrochemical Research Institute (CSIR—CECRI), Karaikudi 630003 Tamil Nadu, India; Academy of Scientific and Industrial Research (AcSIR), Ghaziabad 201002, India;* orcid.org/0000-0001-8059-7043; Email: vganesh@cecri.res.in

Author

Aswathi Mechoor − *Electrodics and Electrocatalysis (EEC) Division, CSIR—Central Electrochemical Research Institute (CSIR—CECRI), Karaikudi 630003 Tamil Nadu, India; Academy of Scientific and Industrial Research (AcSIR), Ghaziabad 201002, India;* orcid.org/0000-0001-6634-3960

Complete contact information is available at: https://pubs.acs.org/10.1021/acsomega.3c05535

Notes

The authors declare no competing financial interest.

■ ACKNOWLEDGMENTS

A.M. acknowledges the financial support received from a DST−INSPIRE Fellowship for the above research work in the form of a Junior Research Fellowship (DST-INSPIRE-JRF). S.B. wishes to acknowledge the funding received from CSIR, India under the Emeritus Scientist Scheme, ref. no. CSIR letter no. 21(1108)-20/EMR-II dt. 21/09/2020. The authors also thank the Central Instrumentation Facility (CIF), CSIR-CECRI for all of the characterizations. CECRI Manuscript Communication Number: CECRI/PESVC/Pubs./2023-090.

■ REFERENCES

(1) Robinson, P. K. Enzymes: principles and biotechnological applications. *Essays Biochem* **2015**, *59*, 1−41.

(2) Wang, J.; et al. Zr(IV)-based metal-organic framework nanocomposites with enhanced peroxidase-like activity as a colorimetric sensing platform for sensitive detection of hydrogen peroxide and phenol. *Environmental Research* **2022**, *203*, 111818.

(3) Singh, S. Nanomaterials Exhibiting Enzyme-Like Properties (Nanozymes): Current Advances and Future Perspectives. *Frontiers in Chemistry* **2019**, *7*, DOI: 10.3389/fchem.2019.00046.

(4) Li, Q.; et al. A High-Efficiency Electrocatalyst for Oxidizing Glucose: Ultrathin Nanosheet Co-Based Organic Framework Assemblies. *ACS Sustainable Chem. Eng.* **2019**, *7* (9), 8986−8992.

(5) Ling, P.; et al. Nanozyme-Modified Metal−Organic Frameworks with Multienzymes Activity as Biomimetic Catalysts and Electrocatalytic Interfaces. *ACS Appl. Mater. Interfaces* **2020**, *12* (15), 17185−17192.

(6) Liu, F.; He, J.; Zeng, M.; Hao, J.; Guo, Q.; Song, Y.; Wang, L. Cu−hemin metal-organic frameworks with peroxidase-like activity as peroxidase mimics for colorimetric sensing of glucose. *J. Nanopart. Res.* **2016**, *18* (5), 106.

(7) K., A.; Vusa, C. S. R.; Berchmans, S. Enhanced peroxidase-like activity of CuWO4 nanoparticles for the detection of NADH and hydrogen peroxide. *Sens. Actuators, B* **2017**, *253*, 723−730.

(8) Wang, S.; et al. Ultrathin ZIF-67 nanosheets as a colorimetric biosensing platform for peroxidase-like catalysis. *Anal. Bioanal. Chem.* **2018**, *410* (27), 7145−7152.
(9) M, A.; Ganesh, V.; Berchmans, S. Metal-Organic Framework-Based Electrode Platforms in the Assembly of Biofuel Cells and Self-Powered Sensors. *ChemElectroChem.* **2022**, *9* (11), e202200276.
(10) Song, D.; et al. Structural modulation of heterometallic metal−organic framework via a facile metal-ion-assisted surface etching and structural transformation. *J. Mol. Liq.* **2021**, *334*, 116073.
(11) Singh, J.; et al. Colorimetric detection of hydrogen peroxide and cholesterol using Fe3O4-brominated graphene nanocomposite. *Anal. Bioanal. Chem.* **2022**, *414* (6), 2131−2145.
(12) Menon, S. S.; et al. Copper- Based Metal-Organic Frameworks as Peroxidase Mimics Leading to Sensitive H2O2 and Glucose Detection. *ChemistrySelect* **2018**, *3* (28), 8319−8324.
(13) Ai, L.; Li, L.; Zhang, C.; Fu, J.; Jiang, J. MIL-53(Fe): A Metal−Organic Framework with Intrinsic Peroxidase-Like Catalytic Activity for Colorimetric Biosensing. *Chemistry − A European Journal* **2013**, *19* (45), 15105−15108.
(14) Li, S.; et al. Enhanced peroxidase-like activity of MOF nanozymes by co-catalysis for colorimetric detection of cholesterol. *J. Mater. Chem. B* **2023**, *11* (33), 7913−7919.
(15) Wang, J.; et al. Bimetallic metal−organic framework for enzyme immobilization by biomimetic mineralization: Constructing a mimic enzyme and simultaneously immobilizing natural enzymes. *Anal. Chim. Acta* **2020**, *1098*, 148−154.
(16) Yang, H.; et al. Doping copper into ZIF-67 for enhancing gas uptake capacity and visible-light-driven photocatalytic degradation of organic dye. *J. Mater. Chem.* **2012**, *22* (41), 21849−21851.
(17) Guo, S.; et al. Syntheses of new zeolitic imidazolate frameworks in dimethyl sulfoxide. *Inorganic Chemistry Frontiers* **2022**, *9* (9), 2011−2015.
(18) Tan, Y.-X.; Wang, F.; Zhang, J. Design and synthesis of multifunctional metal−organic zeolites. *Chem. Soc. Rev.* **2018**, *47* (6), 2130−2144.
(19) Sagar Varangane, C. S. V.; Amritanjali, T. Insitu synthesis of Cu-doped ZIF-8 for efficient photocatalytic water splitting. *Research Square* **2022**, DOI: 10.21203/rs.3.rs-1504980/v1
(20) Kaneti, Y. V.; Dutta, S.; Hossain, M. S. A.; Shiddiky, M. J. A.; Tung, K.-L.; Shieh, F.-K.; Tsung, C.-K.; Wu, K. C.-W.; Yamauchi, Y. Strategies for Improving the Functionality of Zeolitic Imidazolate Frameworks: Tailoring Nanoarchitectures for Functional Applications. *Adv. Mater.* **2017**, *29* (38), 1700213.
(21) Thandavan, K.; et al. Hydrogen peroxide biosensor utilizing a hybrid nano-interface of iron oxide nanoparticles and carbon nanotubes to assess the quality of milk. *Sens. Actuators, B* **2015**, *215*, 166−173.
(22) Zhang, Y.; et al. An Amperometric Hydrogen Peroxide Sensor Based on Reduced Graphene Oxide/Carbon Nanotubes/Pt NPs Modified Glassy Carbon Electrode. *Int. J. Electrochem. Sci.* **2020**, *15* (9), 8771−8785.
(23) Thangavel, B.; Berchmans, S.; Ganesh, V. Hollow spheres of iron oxide as an "enzyme-mimic": preparation, characterization and application as biosensors. *New J. Chem.* **2022**, *46* (9), 4212−4225.
(24) Bos, E. S.; et al. 3,3′,5,5′-Tetramethylbenzidine as an Ames Test Negative Chromogen for Horse-Radish Peroxidase in Enzyme-Immunoassay. *Journal of Immunoassay* **1981**, *2* (3−4), 187−204.
(25) Wu, Y.; et al. A novel reagentless amperometric immunosensor based on gold nanoparticles/TMB/Nafion-modified electrode. *Biosens. Bioelectron.* **2009**, *24* (5), 1389−1393.
(26) Jian, M.; et al. Water-based synthesis of zeolitic imidazolate framework-8 with high morphology level at room temperature. *RSC Adv.* **2015**, *5* (60), 48433−48441.
(27) Sangkaew, P.; et al. Emerging Electrochemical Sensor Based on Bimetallic AuPt NPs for On-Site Detection of Hydrogen Peroxide Adulteration in Raw Cow Milk. *Electrocatalysis* **2022**, *13* (6), 794−806.
(28) Motshakeri, M.; et al. Electrochemical Methods for the Analysis of Milk. *J. Agric. Food Chem.* **2022**, *70* (8), 2427−2449.
(29) Guo, X.; Lin, C.; Zhang, M.; Duan, X.; Dong, X.; Sun, D.; Pan, J.; You, T. 2D/3D Copper-Based Metal-Organic Frameworks for Electrochemical Detection of Hydrogen Peroxide *Frontiers in Chemistry* **2021**, *9*, DOI: 10.3389/fchem.2021.743637.
(30) Sun, S.; et al. Copper-doped ZIF-8 with high adsorption performance for removal of tetracycline from aqueous solution. *J. Solid State Chem.* **2020**, *285*, 121219.
(31) Wongsing, B.; et al. Vanadium-Doped Porous Cobalt Oxide for Its Superior Peroxidase-like Activity in Simultaneous Total Cholesterol and Glucose Determination in Whole Blood Based on a Simple Two-Dimensional Paper-Based Analytical Device. *Anal. Chem.* **2022**, *94* (40), 13785−13794.
(32) Veitch, N. C. Horseradish peroxidase: a modern view of a classic enzyme. *Phytochemistry* **2004**, *65* (3), 249−59.
(33) Hynninen, P. H.; Kaartinen, V.; Kolehmainen, E. Horseradish peroxidase-catalyzed oxidation of chlorophyll a with hydrogen peroxide: characterization of the products and mechanism of the reaction. *Biochim. Biophys. Acta* **2010**, *1797* (5), 531−42.
(34) Jiang, B.; et al. Standardized assays for determining the catalytic activity and kinetics of peroxidase-like nanozymes. *Nat. Protoc.* **2018**, *13* (7), 1506−1520.
(35) Chen, H.; et al. Solution-Phase Synthesis of Platinum Nanoparticle-Decorated Metal-Organic Framework Hybrid Nanomaterials as Biomimetic Nanoenzymes for Biosensing Applications. *ACS Appl. Mater. Interfaces* **2018**, *10* (28), 24108−24115.
(36) Yang, H.; et al. A novel copper-based metal-organic framework as a peroxidase-mimicking enzyme and its glucose chemiluminescence sensing application. *Anal. Bioanal. Chem.* **2021**, *413* (17), 4407−4416.
(37) Mayuri, P.; Saravanan, N.; Senthil Kumar, A. A bioinspired copper 2,2-bipyridyl complex immobilized MWCNT modified electrode prepared by a new strategy for elegant electrocatalytic reduction and sensing of hydrogen peroxide. *Electrochim. Acta* **2017**, *240*, 522−533.
(38) Laviron, E. General expression of the linear potential sweep voltammogram in the case of diffusionless electrochemical systems. *Journal of Electroanalytical Chemistry and Interfacial Electrochemistry* **1979**, *101* (1), 19−28.
(39) Allen, J.; Bard, L. R. F. *Electrochemical Methods Fundamentals and Applications*; Wiley, 2001; p 864.
(40) Jin, G. H.; et al. Graphene oxide-gold nanozyme for highly sensitive electrochemical detection of hydrogen peroxide. *Sens. Actuators, B* **2018**, *274*, 201−209.
(41) Lee, G.-Y.; et al. Chronoamperometry-Based Redox Cycling for Application to Immunoassays. *ACS Sensors* **2018**, *3* (1), 106−112.
(42) Ezenarro, J. J.; et al. Rapid Detection of Legionella pneumophila in Drinking Water, Based on Filter Immunoassay and Chronoamperometric Measurement. *Biosensors* **2020**, *10* (9), 102.
(43) Rani, S.; et al. Sn-MOF@CNT nanocomposite: An efficient electrochemical sensor for detection of hydrogen peroxide. *Environmental Research* **2020**, *191*, 110005.

https://doi.org/10.1021/acsomega.3c05535
ACS Omega 2023, 8, 39636−39650